



Assessing hepatic steatosis by magnetic resonance in potential living liver donors

- Diğdem Kuru Öz¹
 Zeynep Ellik²
 Ayşegül Gürsoy Çoruh¹
 Mehmet Adıgüzel¹
 Mesut Gümüşsoy²
 Saba Kiremitci³
 Onur Elvan Kırımker⁴
 Hale Gökcan²
 Atilla Halil Elhan⁵
 Deniz Balcı⁶
 Berna Savaş³
 Ayşe Erden¹
 Ramazan İdilman^{2,7*}

¹Ankara University Faculty of Medicine, Department of Radiology, Ankara, Türkiye

²Ankara University Faculty of Medicine, Department of Gastroenterology, Ankara, Türkiye

³Ankara University Faculty of Medicine, Department of Pathology, Ankara, Türkiye

⁴Ankara University Faculty of Medicine, Department of General Surgery, Ankara, Türkiye

⁵Ankara University Faculty of Medicine, Department of Biostatistics, Ankara, Türkiye

⁶Bahçeşehir University Faculty of Medicine, Department of General Surgery, İstanbul, Türkiye

⁷Ankara University Hepatology Institute, Ankara, Türkiye

*Ramazan İdilman is a member of the Science Academy (BA).

Corresponding author: Diğdem Kuru Öz

E-mail: digdem_k@hotmail.com

Received 05 February 2024; revision requested 18 March 2024; accepted 17 April 2024.



Epub: 13.05.2024

Publication date: 13.05.2024

DOI: 10.4274/dir.2024.242697

PURPOSE

To determine the accuracy of magnetic resonance imaging-proton density fat fraction (MRI-PDFF) measurements for detecting liver fat content in potential living liver donors and to compare these results using liver biopsy findings.

METHODS

A total of 139 living liver donors (men/women: 83/56) who underwent MRI between January 2017 and September 2021 were included in this analysis retrospectively. The PDFFs were measured using both MR spectroscopy (MRS) and chemical shift-based MRI (CS-MRI) for each donor in a blinded manner.

RESULTS

Significant positive correlations were found between liver biopsy and MRS-PDFF and CS-MRI PDFF in terms of hepatic steatosis detection [$r = 0.701$, 95% confidence interval (CI): 0.604–0.798, $r = 0.654$, 95% CI: 0.544–0.765, $P < 0.001$, respectively]. A weak level correlation was observed between liver biopsy, MRI methods, and vibration-controlled transient elastography attenuation parameters in 42 available donors. Based on receiver operating characteristic (ROC) analysis, MRS-PDFF and CS-MRI PDFF significantly distinguished >5% of histopathologically detected hepatic steatosis with an area under the ROC curve (AUC) of 0.837 ± 0.036 ($P < 0.001$, 95% CI: 0.766–0.907) and 0.810 ± 0.036 ($P < 0.001$, 95% CI: 0.739–0.881), respectively. The negative predictive values (NPVs) of MRS-PDFF and CS-MRI PDFF were 88.3% and 81.3%, respectively. In terms of distinguishing between clinically significant hepatic steatosis ($\geq 10\%$ on histopathology), the AUC of MRS-PDFF and CS-MRI were 0.871 ± 0.034 ($P < 0.001$, 95% CI: 0.804–0.937) and 0.855 ± 0.036 ($P < 0.001$, 95% CI: 0.784–0.925), respectively. The NPVs of MRS-PDFF and CS-MRI were 99% and 92%, respectively.

CONCLUSION

The methods of MRS-PDFF and CS-MRI PDFF provide a non-invasive and accurate approach for assessing hepatic steatosis in potential living liver donor candidates. These MRI PDFF techniques present a promising clinical advantage in the preoperative evaluation of living liver donors by eliminating the requirement for invasive procedures like liver biopsy.

KEYWORDS

Magnetic resonance spectroscopy, proton density fat fraction, chemical shift-based magnetic resonance imaging, liver transplantation, living liver donor, metabolic-associated steatotic liver disease

Metabolic dysfunction-associated steatotic liver disease (MASLD) is a public health problem that affects more than 25% of adults worldwide, causing hepatic and extrahepatic morbidity and mortality.¹⁻³ This disease encompasses a broad spectrum of hepatic conditions, ranging from metabolic dysfunction-associated steatosis, characterized by macrovesicular hepatic steatosis that may be accompanied by mild inflammation, to metabolic dysfunction-associated steatohepatitis, which is additionally characterized by the presence of inflammation and hepatocyte injury, with or without fibrosis, cirrhosis, or hepatocellular carcinoma.^{1,2} MASLD is the most prevalent chronic liver disease, especially in

Western countries, and the proportion of MASLD-related cirrhosis cases among patients on liver transplantation (LT) waiting lists has increased over the years.^{2,3} In Türkiye, the prevalence of MASLD is estimated to be more than 30% in the general population.⁴

Living donor LT (LDLT) is an important mortality-reducing treatment approach for patients with acute and chronic liver failure.^{5,6} The use of LDLT has been gradually increasing due to a lack of available cadaveric liver grafts. Several factors are associated with successful graft organ survival following LT.^{5,7} Donor liver steatosis is critical for successful graft function, graft, and recipient survival in the early post-transplant period, and donor safety.^{6,8} Although <5% hepatic steatosis is universally acceptable for liver organ donation, the inclusion thresholds of the hepatic steatosis fraction may vary among liver transplant centers. Some centers use a threshold of <10%,^{9,10} while others consider <20% or <30% as acceptable for donation.^{11,12} Liver biopsy remains the gold standard diagnostic method for accurately assessing hepatic steatosis. However, due to the invasive nature of biopsy, the potential for sampling errors, and intra- and inter-observer variability, there is a tendency to perform liver biopsies on select donors rather than on all potential donors.^{13,14}

Magnetic resonance (MR)-based fat quantification [proton density fat fraction (PDFF)] is an accurate, non-invasive method for determining and quantifying hepatic steatosis.^{11,15-19} PDFF is the ratio of the MR signal from fat protons to the total MR signal from fat and water protons.²⁰ PDFF is mainly measured using two MRI methods: magnetic resonance spectroscopy (MRS) and chemical shift (CS)-based MRI. MRS data can be acquired efficiently using a high-speed T2-corrected multi-echo sequence during a single-hold breath, minimizing motion arti-

facts. This streamlined approach facilitates the rapid acquisition of metabolic information from a specific voxel region, as described previously.²¹ Conversely, the multi-echo CS-MRI technique, which employs six echoes and is known by various commercial vendor-specific names (e.g., Multi-echo Dixon for Siemens, IDEAL IQ for GE, and mDixon Quant for Philips), can generate a comprehensive PDFF map of the entire liver. As mentioned in one of the initial studies using this technique, there is a close correlation between liver biopsy results and CS-MRI PDFF in patients with non-alcoholic fatty liver disease.²² The most significant advantages of this technique include the ability to obtain a PDFF map for the entire liver and perform measurements in different liver regions. In contrast, MRS is limited to sampling a voxel area of a few cm³. MRI is also used in donor hepatic vascular and biliary system anatomy examination.

Increasingly prevalent in the general population, MASLD poses a significant problem in LDLT, leading to morbidity and mortality in both the recipient and the donor. MRS and CS-MRI are proven techniques for assessing and quantifying liver fat presence. However, data regarding the diagnostic accuracy and utility of MRI-based fat quantification in transplant settings is limited. Accordingly, this study aims to determine the accuracy of MRS-PDFF and CS-MRI PDFF measurements for detecting and quantifying the liver fat content in potential living liver donors and to compare these results with liver biopsy findings.

an MRI examination between January 2017 and September 2021. Six donors with suboptimal examinations due to artifacts were excluded from the investigation to ensure the reliability of the data analysis (Figure 1 represents patient accrual). The median time interval between MR and liver biopsy was 12 days (range: 1–30 days). Data were collected from outpatient visit charts. Percutaneous liver biopsy was performed in living liver donors who had abnormal liver injury and/or cholestatic liver tests, obesity, or hepatic steatosis detected by ultrasonography. This study was approved by the Ankara University Human Research Ethics Committee (date: October 2021, decision no: I5-365-21). Written informed consent was waived due to the study's retrospective design.

Serum alanine aminotransferase (ALT), aspartate aminotransferase (AST), gamma-glutamyl transpeptidase (GGT), alkaline phosphatase, bilirubin, fasting glucose, lipid profiles, and complete blood cell counts were measured in our central laboratory.

Magnetic resonance imaging technique

The MRI scans were performed using a 1.5 Tesla MRI device (Aera, Siemens Healthcare, Erlangen, Germany) with an 18-channel body matrix coil and a 32-channel spine matrix coil, utilizing eight channels. In liver donor candidates, in addition to the standard non-contrast abdomen MRI protocol, the LiverLab program provided by the vendor was used to determine and quantify the presence of iron and fat accumulation in the liver. The LiverLab program integrated into liver MRI comprised three sequences: T1 volumetric interpolated breath-hold examination (VIBE) e-Dixon, VIBE q-dixon, and HISTO. The VIBE q-dixon is a single-breath-hold sequence comprising six echoes, which en-

Main points

- The magnetic resonance spectroscopy-proton density fat fraction (MRS-PDFF) and chemical shift-based-MR imaging (CS-MRI) PDFF methods are effective, non-invasive techniques for assessing hepatic steatosis in living liver donor candidates.
- MRI methods, with their high negative predictive value, can eliminate the need for liver biopsy by detecting clinically significant hepatic steatosis.
- The MRS-PDFF and CS-MRI PDFF methods exhibit a high level of correlation in evaluating hepatic steatosis, suggesting that they can be used interchangeably.

Methods

Participants

This retrospective study comprised 145 potential living liver donors who underwent

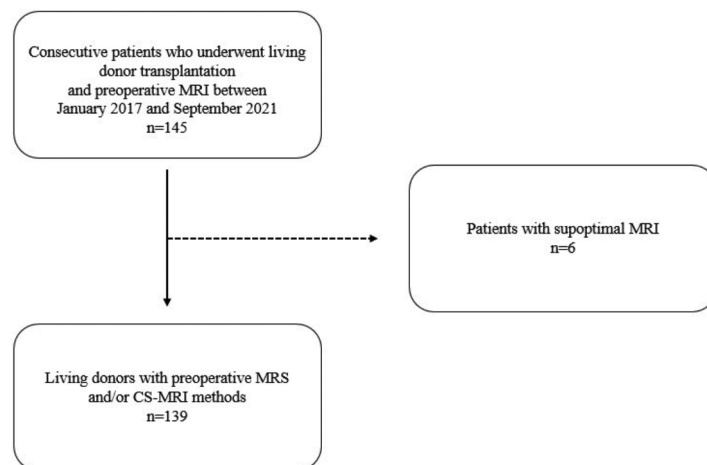


Figure 1. Flowchart summarizing patient accrual. MRI, magnetic resonance imaging; MRS, magnetic resonance spectroscopy; CS, chemical shift.

ables the acquisition of volumetric PDFF and R2* maps, forming the basis of CS-MRI. The HISTO sequence, forming the basis of MRS, was obtained using a 15-second breath-hold T2-corrected multi-echo stimulated echo acquisition mode sequence, utilizing a single voxel of 3 × 3 × 3 cm dimensions. The MRS data were acquired from a single voxel positioned by an experienced MR technician in a homogenous area away from vascular and biliary structures and liver edges in the right lobe during the scan.

Image analysis

The values of MRS PDFF were obtained from the report generated by the HISTO sequence provided by the manufacturer (calculated using Siemens software). Then, CS-MRI PDFF was performed on a dedicated workstation (Syngo., Siemens Healthcare), using the volumetric FF map transferred to it. The measurements of PDFF were conducted by two abdominal radiologists, with 10 (D.K.Ö.) and 2 (M.A.) years of experience. Measurements were obtained by placing three 200–300 mm² regions of interest (ROI) in at least 3 sections of the FF map at the level of the mid-right hepatic lobe (Figure 2). The radiologists conducting the measurements were unaware of the clinical data. Inconsistent measurement results were reevaluated until a consensus was reached. In cases of similar results, measurements performed by experienced radiologists were evaluated statistically. The ROIs were positioned within the homogeneous parenchymal area, avoiding vascular and biliary structures and the liver edges. The average PDFF values for each participant were calculated.

Transient elastography

Hepatic steatosis was also measured using a FibroScan probe (Echosens, Paris,

France) with an M or XL probe to cater to patients with different body types. All measurements were performed by one of the authors (Z.E.). Patients were examined after fasting overnight. The FibroScan probe was placed in the appropriate intercostal space window on the anterior axillary line. At least 10 valid measurements were obtained within 5–10 minutes. The median ratio of 10 successive measurements to the interquartile range was <30%. Simultaneously, vibration-controlled transient elastography (VCTE) was used to measure the controlled attenuation parameter (CAP) (dB/m) and liver stiffness (kPa). Morbidly obese patients [body mass index (BMI) >40 kg/m²] and severely underweight patients (BMI <16 kg/m²), patients with ascites, and patients with moderate and severe cholestasis were excluded.

Histological assessments

Two pathologists (S.K., B.S.) blinded to the clinical and biochemical data re-evaluated all liver biopsy specimens. The histological features of the samples were interpreted using the criteria of Brunt et al.²³ Hepatocellular steatosis was graded on a scale of 0–3 based on the percentage of hepatocytes: 0 = <5%, 1 = 5%–33%, 2 = 33%–66%, and 3 = >66%.

Definitions

The primary endpoint was the assessment of hepatic steatosis using MRI methods, MRS-PDFF, and CS-MRI PDFF. The secondary endpoint was to compare the MRI results with the liver biopsy findings.

Statistical analysis

Descriptive statistics were summarized as percentages for categorical variables, mean and standard deviations for normally

distributed continuous variables, and median, minimum, and maximum for ordinal and non-normally distributed continuous variables. Spearman's correlation coefficient analysis was performed to determine the degree of association between PDFF and histopathology. Bootstrapping was used to estimate confidence intervals (CIs) for Spearman's correlation coefficient. Intra-group comparison of categorical variables was performed using the McNemar test. Receiver operating characteristic (ROC) curves were used to describe and compare the performance of the diagnostics value of the MRI methods. Youden's index was used to determine the optimal cut-off value. The PDFF measurement results were compared with the liver biopsy results. The significance level was established as $\alpha = 0.05$, and the R programming language 4.3.1 was used for statistical analysis.

Results

A total of 139 potential living liver donors (men/women: 83/56) were included in this study. The median age of the donors was 31.0 years (range: 17–59 years). The median BMI was 24.9 kg/m² (range: 17.6–33.2 kg/m²), 40% of the patients were overweight (25–29.9 kg/m²), and 18% were obese (≥ 30 kg/m²). Of the donors, 35% had diabetes mellitus, and 28% had hypertension. The median serum ALT level was 18 U/L (range: 6–56 U/L), the median AST level was 20 U/L (range: 10–4 U/L), and the median GGT level was 20 U/L (range: 7–95 U/L). The donors' clinical data and laboratory values are presented in Table 1.

Hepatic steatosis was detected in 54 donors in the liver biopsy assessment. A total of 50 (36%) donors had grade 1 steatosis, 3 (2%) had grade 2 steatosis, and 1 (1%) had grade 3 steatosis, whereas 85 (61%) had no steatosis. Using the threshold values obtained from ROC analysis with MRS and CS-MRI methods, 9 out of 54 donors confirmed to have hepatic steatosis histopathologically showed no steatosis with MRS, while 12 showed no steatosis with CS-MRI. While there were 7 cases with no detected steatosis by both MRI methods, the PDFF value of 1 case using MRS and 2 cases using CS-MRI could not be obtained due to artifacts. In 5 out of 7 cases, histopathologically, there was minimal steatosis at the lower limit (5%), whereas in the remaining cases, there was mild steatosis (8%–10%).

The mean MRS-PDFF and CS-MRI PDFF were $5.8\% \pm 3.9\%$ and $4.1\% \pm 3.9\%$, respec-

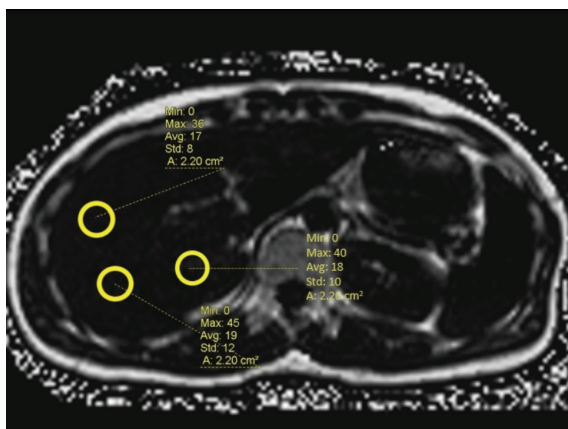


Figure 2. The CS-MRI PDFF measurements were obtained by averaging the values of circular ROIs placed at the level of the mid-right hepatic lobe of the liver in at least three different areas, each measuring 200–300 mm², on the FF map. CS-MRI, chemical shift-magnetic resonance imaging; PDFF, proton density fat fraction; ROI, regions of interest; FF, fat fraction.

tively. Significant positive correlations were found between liver biopsy and MRS-PDFF and CS-MRI-PDFF in terms of hepatic steatosis detection ($r = 0.701$, 95% CI: 0.604–0.798 and $r = 0.654$, 95% CI: 0.544–0.765, $P < 0.001$, respectively). Additionally, VCTE was performed on 42 available donors. The mean CAP was 248.4 ± 60.0 dB/m. A weak-moderate correlation was observed between liver biopsy, MRS-PDFF, CS-MRI PDFF, and VCTE CAP in terms of hepatic steatosis detection ($r = 0.616$, $P < 0.001$, 95% CI: 0.402–0.831, and $r = 0.513$, $P < 0.001$, 95% CI: 0.254–0.772, and

$r = 0.351$, $P = 0.017$, 95% CI: 0.062–0.640, respectively) (Table 2).

An ROC analysis was performed to distinguish between clinically significant and non-significant hepatic steatosis. Significantly, MRS-PDFF and CS-MRI PDFF distinguished $>5\%$ of histopathologically detected patients of hepatic steatosis with an area under the ROC curve (AUC) of 0.837 ± 0.036 (95% CI: 0.766–0.907) and 0.810 ± 0.036 (95% CI: 0.739–0.881), $P = 0.345$ (Table 3, Figure 3a). The optimal thresholds for MRS-PDFF and CS-MRI were 4.65% and 3.45%,

respectively. The sensitivities of MRS-PDFF and CS-MRI were 83.3% (95% CI: 71.3%–91.0%) and 74.1% (95% CI: 61.1%–83.9%, $P = 0.063$), respectively, whereas the specificities of MRS-PDFF and CS-MRI were 80.0% (95% CI: 70.3%–87.1%) and 71.8% (95% CI: 61.4%–80.2%, $P = 0.118$), respectively. The negative predictive values (NPVs) of MRS-PDFF and CS-MRI PDFF were 88.3% (95% CI, 79.3%–93.7%) and 81.3% (95% CI: 71.1%–88.5%), respectively. In terms of distinguishing clinically significant hepatic steatosis ($\geq 10\%$ on histopathology), the AUCs of MRS-PDFF and CS-MRI were 0.871 ± 0.034 , (95% CI: 0.804–0.937, $P < 0.001$) and 0.855 ± 0.036 , (95% CI: 0.784–0.925, $P < 0.001$), respectively (Table 3, Figure 3b). The cut-off values were 4.65% and 3.95%, respectively. The sensitivity of MRS-PDFF was significantly better than that of CS-MRI PDFF for distinguishing significant hepatic steatosis ($\geq 10\%$ on histopathology) [97.2% (95% CI: 85.8%–99.5%) vs. 80.6% (95% CI: 0.65.0%–90.2%), $P = 0.031$]. The specificities of these MRI methods were 73.8% (95% CI: 64.5%–81.3%) and 78.6% (95% CI: 69.8%–85.5%, $P = 0.302$), respectively.

Table 1. Clinical data and laboratory values of donors			
Demographics	n, %	Mean \pm SD	Median (min–max)
Age (years)			31 (17–59)
Men	83 (59.7)		
Women	56 (40.3)		
BMI	133 (95.7)	24.8 \pm 3.11	
Overweight and obesity	80 (58)		
Laboratory tests			
Serum ALT levels	139 (100)		18 (6–56)
Serum AST levels	139 (100)		20 (10–44)
Serum ALP levels	139 (100)		78 (28–208)
Serum GGT levels	139 (100)		20 (7–95)
Total bilirubin levels	139 (100)		0.59 (0.20–3.10)
Albumin levels	139 (100)	45.5 \pm 3.11	
Thrombocyte count	139 (100)		268 (141–548)
INR	139 (100)		1.02 (0.82–1.30)
LDL levels	137 (98.6)	114.6 \pm 34.7	
HDL levels	137 (98.6)		45 (29–80)
Total cholesterol level	136 (97.8)	184.5 \pm 40.5	
Non-HDL levels	136 (97.8)	137.1 \pm 39.7	
Triglyceride levels	137 (98.6)		99 (18–606)
VLDL levels	137 (98.6)		20 (3–121.2)
VCTE-CAP	42 (30.2)	248.4 \pm 60.0	

SD, standard deviation; min, minimum; max, maximum; BMI, body mass index; ALT, alanine transaminase; AST, aspartate transaminase; ALP, alkaline phosphatase; GGT, gamma-glutamyl transferase; INR, international normalized ratio; LDL, low-density lipoprotein cholesterol; HDL, high-density lipoprotein cholesterol; VLDL, very low-density lipoprotein cholesterol; VCTE-CAP, vibration controlled transient elastography-controlled attenuation parameter.

Table 2. The correlation analysis between histopathology and MRI PDFF methods and VCTE CAP						
	Histopathology Fat content		MRS PDFF		CS-MRI PDFF	
	r	P	r	P	r	P
MRS PDFF	0.704 (n = 136)	<0.001*				
CS-MRI PDFF	0.690 (n = 125)	<0.001*	0.823	<0.001*		
VCTE CAP	0.616 (n = 42)	<0.001*	0.566	<0.001*	0.379	0.014*

*Statistically significant. MRS, magnetic resonance spectroscopy; PDFF, proton density fat fraction; CS-MRI, chemical shift-magnetic resonance imaging; VCTE-CAP, vibration-controlled transient elastography-controlled attenuation parameter.

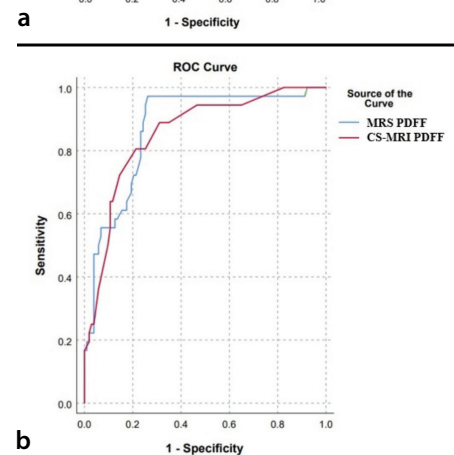
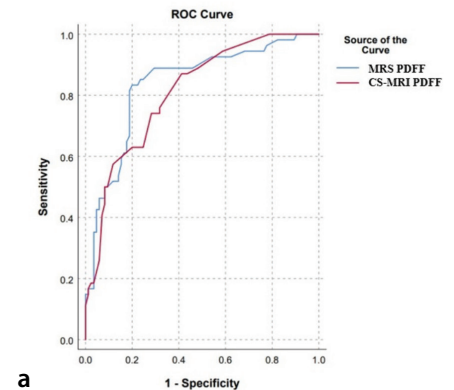


Figure 3. ROC curve for MRS-PDFF and CS-MRI PDFF for the detection of hepatic fat content, (a) $>5\%$ on histopathology, and (b) $\geq 10\%$ on histopathology. ROC, receiver operating characteristic; MRS, magnetic resonance spectroscopy; PDFF, proton density fat fraction; CS-MRI, chemical shift-magnetic resonance imaging.

The NPVs of MRS-PDF and CS-MRI were 98.7% (95% CI: 93.0%–99.8%) and 92% (95% CI: 84.5%–96.1%), respectively.

Discussion

This large-sample study compared the accuracy of MRI techniques in assessing hepatic fat content in potential living liver donors. It was found that MRS-PDF and CS-MRI PDFF accurately assessed hepatic fat content and were strongly positively correlated with evaluating hepatic steatosis by liver biopsy. However, VCTE showed a weak-moderate correlation with liver biopsy assessment and MRI methods.

Steatotic liver graft has been associated with an increased risk of graft dysfunction or graft failure, especially in the early post-transplant period, mainly due to ischemia-reperfusion injury.⁸ There are still unanswered questions regarding what constitutes acceptable risk concerning the level of fat content in living liver donors. The prevalence of MASLD is increasing globally, and LDLT is a vital therapeutic option for managing end-stage liver disease. Therefore, it is crucial to understand how to effectively assess donor liver fat content. Several previous studies have investigated the role of MRI in liver fat content assessment in both transplant and non-transplant settings.^{15,24-26} A meta-analysis reported that MRI-PDF demonstrated 89% specificity and 84% sensitivity in detecting donor candidates with >5% hepatic steatosis, as determined by liver biopsy.²⁷ In addition, in a study of 32 potential liver donors, MRS distinguished donors with significant hepatic steatosis designated as >10% on histopathological examination. The investigators concluded

that CS-MRI and MRS would eliminate the need for liver biopsy.²⁸ In this study, MRS-PDF and CS-MRI PDFF could distinguish between liver donors with/without clinically significant hepatic steatosis (>5%) on histopathological examination, with high NPVs. The accuracy and the NPVs of the MRI methods were increased when distinguishing donors with >10% hepatic steatosis on histopathology.

This study found cut-off values for MRS-PDF and CS-MRI PDFF of 4.65% and 3.45%, respectively, for distinguishing >5% of hepatic steatosis, as detected by liver biopsy. These values improved the identification of histopathological liver fat content with a high NPV. These findings suggest that living donor candidates with <4.65% PDFF on MRI could potentially qualify as living liver donors. Previous studies reported no significant differences between the two MRI methods for identifying hepatic fat content.²¹ According to Idilman et al.²⁹, in scanners where one of the two software tools is not available, the hepatic steatosis percentage can be accurately determined using the alternative method currently in place. However, having both methods in the standard MRI protocol for liver donors offers several advantages. The results of both methods can be used to corroborate each other. For instance, in cases of heterogeneous fat deposition or misplacement of the voxel, MRS may yield incorrect results. Furthermore, in the case of fat-water swapping artifacts, the PDFF cannot be obtained through CS-MRI. In such cases, PDFF can be determined using MRS. The increase in the correlation with histopathology when both MRI methods are used to complement each other, despite miss-

ing PDFF data, is the strongest evidence of the advantages of using both MRI methods with donors.

The VCTE CAP values exhibited a relatively weak correlation with the histopathological findings. Previous studies have reported a VCTE moderate correlation between VCTE CAP and MRI-PDF.^{30,31} This study confirms previous studies demonstrating a weak-moderate correlation between CAP and liver biopsy, as well as MRI methods assessing hepatic steatosis.

While this study demonstrated a correlation between histopathology and MRI methods in identifying hepatic fat content, it possesses several notable limitations. First, it relied on retrospective observational data from a tertiary referral center. Moreover, there is a potential for bias related to the participants' data and confounding factors. Additionally, although all candidates underwent extensive investigation before donation and were deemed healthy, the donor's hepatic iron content was not measured, potentially impacting fat quantification with MRI. Despite being costly techniques for routine practice, they should be acknowledged as cost-effective methods in evaluating patients before complex surgical procedures such as LT, which carry high morbidity and mortality rates in tertiary referral healthcare centers.

In conclusion, MRS-PDF and CS-MRI PDFF accurately assess the presence and grade of hepatic fat content in potential living liver donor candidates. MRI is a non-invasive and valuable tool for use in the liver donor selection process for LDLT.

n=139	> 5% steatosis			>10 steatosis		
	MRS	CS-MRI	P	MRS	CS-MRI	P
Cutt-off FF (%)	4.65	3.45		4.65	3.95	
AUC	0.837 ± 0.036	0.810 ± 0.036		0.871 ± 0.034	0.855 ± 0.036	
95% CI	(0.766–0.907)	(0.739–0.881)	0.345	(0.804–0.937)	(0.784–0.925)	0.508
P value	<0.001	<0.001		<0.001	<0.001	
Sensitivity	0.833	0.741		0.972	0.806	
95% CI	(0.712–0.910)	(0.611–0.839)	0.063	(0.858–0.995)	(0.650–0.902)	0.031
Specificity	0.800	0.718		0.738	0.786	
95% CI	(0.703–0.871)	(0.615–0.803)	0.118	(0.645–0.813)	(0.698–0.855)	0.302
PPV	0.726	0.625		0.565	0.569	
95% CI	(0.604–0.821)	(0.503–0.734)		(0.441–0.681)	(0.433–0.695)	
NPV	0.883	0.814		0.987	0.920	
95% CI	(0.792–0.937)	(0.711–0.886)		(0.930–0.998)	(0.845–0.961)	
Accuracy	0.813	0.727		0.799	0.791	

MRI, magnetic resonance imaging; FF, fat fraction; AUC, area under the curve; CI, confidence interval; PPV, positive predictive value; MRS, magnetic resonance spectroscopy; CS, chemical shift; NPV, negative predictive value.

Conflict of interest disclosure

The authors declared no conflicts of interest.

References

1. Rinella ME, Lazarus JV, Ratziu V, et al. A multisociety Delphi consensus statement on new fatty liver disease nomenclature. *Ann Hepatol*. 2023;101133. [CrossRef]
2. Younossi ZM, Koenig AB, Abdelatif D, Fazel Y, Henry L, Wymer M. Global epidemiology of nonalcoholic fatty liver disease—meta-analytic assessment of prevalence, incidence, and outcomes. *Hepatology*. 2016;6473-6484. [CrossRef]
3. Wong RJ, Aguilar M, Cheung R, et al. Nonalcoholic steatohepatitis is the second leading etiology of liver disease among adults awaiting liver transplantation in the United States. *Gastroenterology*. 2015;148:547-555. [CrossRef]
4. Yilmaz Y, Yilmaz N, Ates F, et al. The prevalence of metabolic-associated fatty liver disease in the Turkish population: a multicenter study. *Hepatol Forum*. 2021;21:2:37-42. [CrossRef]
5. Yilmaz S, Kayaalp C, Ara C, et al. Single-center analysis of the first 304 living-donor liver transplantations in 3 years. *Hepatogastroenterology*. 2013;60:1105-1109. [CrossRef]
6. Chen CL, Fan ST, Lee SG, Makuuchi M, Tanaka K. Living-donor liver transplantation: 12 years of experience in Asia. *Transplantation*. 2003;75(3 Suppl):6-11. [CrossRef]
7. Cheng YF, Chen CL, Lai CY, et al. Assessment of donor fatty livers for liver transplantation. *Transplantation*. 2001;71:1221-1225. [CrossRef]
8. Perez-Daga JA, Santoyo J, Suárez MA, et al. Influence of degree of hepatic steatosis on graft function and postoperative complications of liver transplantation. *Transplant Proc*. 2006;38:2468-2470. [CrossRef]
9. Sharma A, Ashworth A, Behnke M, Cotterell A, Posner M, Fisher RA. Donor selection for adult-to-adult living donor liver transplantation: well begun is half done. *Transplantation*. 2013;95:501-506. [CrossRef]
10. Trotter JF, Campsen J, Bak T, et al. Outcomes of donor evaluations for adult-to-adult right hepatic lobe living donor liver transplantation. *Am J Transplant*. 2006;6:1882-1889. [CrossRef]
11. Gallegos-Orozco JF, Silva AC, Batheja MJ, et al. Magnetic resonance elastography can discriminate normal vs. abnormal liver biopsy in candidates for live liver donation. *Abdom Imaging*. 2015;40:795-802. [CrossRef]
12. Kim SH, Lee JM, Han JK, et al. Hepatic macrosteatosis: predicting appropriateness of liver donation by using MR imaging—correlation with histopathologic findings. *Radiology*. 2006;240:116-129. [CrossRef]
13. Ratziu V, Charlotte F, Heurtier A, et al. Sampling variability of liver biopsy in nonalcoholic fatty liver disease. *Gastroenterology*. 2005;128:1898-1906. [CrossRef]
14. Myers RP, Fong A, Shaheen AA. Utilization rates, complications and costs of percutaneous liver biopsy: a population-based study including 4275 biopsies. *Liver Int*. 2008;28:705-712. [CrossRef]
15. Hwang I, Lee JM, Lee KB, et al. Hepatic steatosis in living liver donor candidates: preoperative assessment by using breath-hold triple-echo MR imaging and 1H MR spectroscopy. *Radiology*. 2014;271:730-738. [CrossRef]
16. Loomba R, Adams LA. Advances in non-invasive assessment of hepatic fibrosis. *Gut*. 2020;69:1343-4352. [CrossRef]
17. Hsu C, Caussy C, Imajo K, et al. Magnetic resonance vs transient elastography analysis of patients with nonalcoholic fatty liver disease: a systematic review and pooled analysis of individual participants. *Clin Gastroenterol Hepatol*. 2019;17:630-637. [CrossRef]
18. Cui J, Heba E, Hernandez C, et al. Magnetic resonance elastography is superior to acoustic radiation force impulse for the diagnosis of fibrosis in patients with biopsy-proven nonalcoholic fatty liver disease: A prospective study. *Hepatology*. 2016;63:453-461. [CrossRef]
19. Park CC, Nguyen P, Hernandez C, Bettencourt R, Ramirez K, Fortney L, et al. Magnetic resonance elastography vs transient elastography in detection of fibrosis and noninvasive measurement of steatosis in patients with biopsy-proven nonalcoholic fatty liver disease. *Gastroenterology*. 2017;152(3):598-607.e2. [CrossRef]
20. Yokoo T, Serai SD, Pirasteh A, et al. Linearity, bias, and precision of hepatic proton density fat fraction measurements by using MR imaging: a meta-analysis. *Radiology*. 2018;286:486-498. [CrossRef]
21. Rastogi R, Gupta S, Garg B, Vohra S, Wadhawan M, Rastogi H. Comparative accuracy of CT, dual-echo MRI and MR spectroscopy for preoperative liver fat quantification in living related liver donors. *Indian J Radiol Imaging*. 2016;26:5-14. [CrossRef]
22. Idilman IS, Aniktar H, Idilman R, et al. Hepatic steatosis: quantification by proton density fat fraction with MR imaging versus liver biopsy. *Radiology*. 2013;267:767-775. [CrossRef]
23. Brunt EM, Kleiner DE, Carpenter DH, et al. NAFLD: reporting histologic findings in clinical practice. *Hepatology*. 2021;73:2028-2038. [CrossRef]
24. Tang A, Tan J, Sun M, et al. Nonalcoholic fatty liver disease: MR imaging of liver proton density fat fraction to assess hepatic steatosis. *Radiology*. 2013;267:422-431. [CrossRef]
25. Chiang HJ, Chang WP, Chiang HW, et al. Magnetic resonance spectroscopy in living-donor liver transplantation. *Transplant Proc*. 2016;48:1003-1006. [CrossRef]
26. Chaudhary A, Sood G, Kumar N, et al. Validation of accuracy of non-invasive imaging methods (magnetic resonance imaging (MRI) fat fraction calculation and computed tomography (CT) liver attenuation index) for hepatic graft fat quantification in living liver transplant donors. *Ann Transplant*. 2021;26:e933801. [CrossRef]
27. Zheng D, Guo Z, Schroder PM, et al. Accuracy of MR imaging and MR spectroscopy for detection and quantification of hepatic steatosis in living liver donors: a meta-analysis. *Radiology*. 2017;282:92-102. [CrossRef]
28. Satkunasingham J, Nik HH, Fischer S, et al. Can negligible hepatic steatosis determined by magnetic resonance imaging-proton density fat fraction obviate the need for liver biopsy in potential liver donors? *Liver Transpl*. 2018;24:470-477. [CrossRef]
29. Idilman IS, Keskin O, Celik A, et al. A comparison of liver fat content as determined by magnetic resonance imaging-proton density fat fraction and MRS versus liver histology in non-alcoholic fatty liver disease. *Acta Radiol*. 2016;57:271-278. [CrossRef]
30. Zhuang RH, Weinstock AK, Ganesh S, et al. Characterization of hepatic steatosis using controlled attenuation parameter and MRI-derived proton density fat fraction in living donor liver transplantation. *Clin Transplant*. 2022;36:e14786. [CrossRef]
31. Ferraioli G, Maiocchi L, Savietto G, et al. Performance of the attenuation imaging technology in the detection of liver steatosis. *J Ultrasound Med*. 2021;40:1325-1332. [CrossRef]